frontiers | Frontiers in Chemistry

ORIGINAL RESEARCH
published: 31 May 2022
doi: 10.3389/fchem.2022.916092

CeO_2 Structure Adjustment by H_2O *via* the Microwave–Ultrasonic Method and Its Application in Imine Catalysis

Xijiang Chang[1], *Huihui Ding*[2] *and Jingxia Yang*[2]*

[1]College of Science, Donghua University, Shanghai, China, [2]College of Chemistry and Chemical Engineering, Shanghai University of Engineering Science, Shanghai, China

CeO_2 with fusiform structures were prepared by the combined microwave–ultrasonic method, and their morphologies and surface structure were changed by simply adding different amounts of H_2O (1–5 ml) to the precursor system. The addition of H_2O changed the PVP micelle structure and the surface state, resulting in CeO_2 with a different specific surface area (64–111 $m^2\ g^{-1}$) and Ce^{3+} defects (16.5%–28.1%). The sample with 2 ml H_2O exhibited a high surface area (111.3 $m^2{\cdot}g^{-1}$) and relatively more surface defects (Ce^{3+}%: 28.1%), resulting in excellent catalytic activity (4.34 mmol $g^{-1}\ h^{-1}$).

Keywords: CeO_2, catalyst, imine synthesis, microwave synthesis, microwave-ultrasonic combined method

OPEN ACCESS

Edited by:
Xijun Wei,
Southwest University of Science and Technology, China

Reviewed by:
Yi Liu,
Zhejiang University, China
Shifei Kang,
University of Shanghai for Science and Technology, China

***Correspondence:**
Jingxia Yang
yjx09tj@foxmail.com
jxyang@sues.edu.cn

Specialty section:
This article was submitted to Inorganic Chemistry, a section of the journal Frontiers in Chemistry

Received: *08 April 2022*
Accepted: *25 April 2022*
Published: *31 May 2022*

Citation:
Chang X, Ding H and Yang J (2022) CeO_2 Structure Adjustment by H_2O via the Microwave–Ultrasonic Method and Its Application in Imine Catalysis. Front. Chem. 10:916092. doi: 10.3389/fchem.2022.916092

HIGHLIGHTS

1. Fusiform-like CeO_2 was prepared by the combined microwave–ultrasonic method.
2. 1–5 ml H_2O in the precursor can influence the morphology, surface area, and Ce^{3+}% of the CeO_2 catalyst.
3. H_2O changed the PVP micelle structure, leading to modulation of the CeO_2 surface state.
4. For imine synthesis, CeO_2 with 2 ml H_2O showed 2-times higher activity than the control without H_2O.

INTRODUCTION

Imine compounds are important intermediates for many biological, agricultural, and pharmaceutical compounds, such as alkaloids, membered heterocycles, and nitrogen heterocycles (Martin, 2009; Kaldas et al., 2017); thus, it is of great importance to develop a new synthesis approach for imine. CeO_2 is a new promising catalyst for imine synthesis, which can overcome the problems caused by traditional acid/base catalysts (Tamura and Tomishige, 2015) and bring a lot of advantages, such as mild synthesis conditions and fast separation. Many research studies have focused on CeO_2 application in imine synthesis (Geng et al., 2016; Long et al., 2019a; Long et al., 2019b; Cao et al., 2020; Rizzuti et al., 2020; Tamura and Tomishige, 2020), and it has been reported that CeO_2 morphologies can greatly influence the catalytic activity for imine synthesis (Zhang et al., 2017; Yang et al., 2018; Zhang et al., 2018; Yang et al., 2020a; Yang et al., 2020b), which have a close relationship with the CeO_2 specific surface area and Ce^{3+} defects.

The preparation approach can effectively change the structure of CeO_2, especially using the microwave method. Microwaves can heat the target solution by interacting with the solution molecules; thus, the solution can be heated fast and uniformly, which can effectively improve the product quality (Reddy et al., 2012; Li et al., 2021; Ma et al., 2021). Besides, other energies, such as

UV-light and ultrasonic force, can work together with microwaves to achieve a new CeO_2 material structure *via* the Multifunctional Microwave Synthesis and Extraction Workstation (Yang et al., 2020a). Ultrasonic force is a kind of energy-accumulated mechanical vibration waves with thermal effect, mechanical effect, and cavitation effect (Thompson and Doraiswamy, 2000; Dalas, 2001; Shen, 2009), which can be used to accelerate the reaction rate and improve particle dispersion during material synthesis.

Microwave- or ultrasonic-assisted technology for CeO_2 synthesis has developed very rapidly in recent years (Leonelli and Mason, 2010; Phuruangrat et al., 2017; Zhao et al., 2018; Mousavi-Kamazani and Ashrafi, 2020; Chen et al., 2021; Zhai et al., 2021), and it has been found that different CeO_2 structures were obtained by using different energy inputs with the same solution (Yang et al., 2020a). Applying microwaves and ultrasonic waves together to the same solution can synthesize materials with a novel structure. In this way, the heat and mass can be transferred much better, and a new material structure can be achieved by changing the solution very slightly.

In this work, a series of CeO_2 nanomaterials was synthesized by a combined microwave–ultrasonic method. Different CeO_2 structures can be achieved only by changing the amount of deionized water in the solvent. The obtained CeO_2 exhibited different catalytic activities for imine synthesis, and their structures were further characterized by XRD, IR, SEM, XPS, and BET to figure out the materials' structure and the reason behind it.

EXPERIMENTAL

Synthesis of CeO_2

All chemicals were provided by Adamas Reagents and used as received. The combined microwave-ultrasonic method was used to synthesis CeO_2, using $Ce(NO_3)_3{\cdot}6H_2O$ as the starting precursor, PVP as the structure directing agent, and acetic acid (HAC) as the mineralizer. The solvents were formed by ethylene glycol (EG) and DI-H_2O, with a fixed total volume of 35.0 ml. The synthesis procedures were all the same; only the solvent content was changed by using different amounts of H_2O, as shown in **Table 1**. The typical synthesis procedure was described using CeO_2-H2 as an example. $Ce(NO_3)_3{\cdot}6H_2O$ (2.17 g) was dissolved into the mixed solvent (33 ml EG + 2 ml DI-H_2O) in a three-neck flask; then PVP (1.00 g) was added, and the resultant solution was stirred for 2 h. Finally, HAC (2.0 ml) was dropwise added, and the solution was further stirred for 15 min. Then the three-neck flask was transferred to a Multifunctional Microwave Synthesis and Extraction Workstation [Uwave-2000 from SINEO Microwave Chemistry Technology (China) Co. Ltd.] using microwave and ultrasonic force as the energy input, as shown in **Figure 1A**. The heating program is shown in **Figure 1B**, where the temperature is maintained at 100°C for 5 min and at 180°C for 12 min. After cooling naturally, the solids were centrifuged, washed by ethanol and DI-H_2O four times, and dried in an oven (80°C) overnight. After that, they were calcined at 500°C (2°C/min) for 1 h in air to remove surface organic residues. In the sample name CeO_2-H*x*, *x* is the volume of DI-H_2O added to the solvent.

Structure Characterization

The XRD patterns were acquired using a Shimadzu (Japan) D/Max-2500 diffractometer (nickel-filtered CuKα radiation). The morphologies of the CeO_2 samples were observed using a scanning electron microscope (SEM, Hitachi S-8000, Japan) in the secondary electron scattering mode at 5 kV. N_2 adsorption/desorption was measured at 77 K by using a Micromeritics ASAP 2020 instrument, and all samples were degassed at 120°C for at least 5 h before testing. X-ray photoelectron spectra (XPS) were recorded using a Thermo Fisher ESCALAB 250 xi (England) using AlKα radiation (1,486.6 eV).

CeO_2 as Catalyst for Imine Synthesis

Calcined CeO_2 (50 mg) was added to a mixture of benzyl alcohol (10 mmoL) and aniline (20 mmoL). The resulting mixtures were stirred vigorously at 500 rpm at 50°C. After a certain time (at least 2 h), the imine product was analyzed using HPLC (Shimadzu LC-20AT, Japan) equipped with a Hypersil ODS C18 column (5 μm in a size of 4.6 mm × 250 mm), and the mobile phase was methanol: water = 8:2. In order to compare with the other reactions, the reaction rates are given as the amount of imine formation per hour per catalyst mass (mmol h^{-1} g^{-1}).

RESULTS AND DISCUSSIONS

The x-ray diffraction (XRD) patterns of all samples are shown in **Figure 2A**. Typical CeO_2 crystalline phases (JCPDF No: 34-0394) appeared for all samples, which were prepared by the combined microwave–ultrasonic method and calcined at 500°C in air for 1 h, similar to the one reported before (Yang et al., 2021), but the crystalline particle sizes were different when calculated by Scherrer equations based on the strongest (111) peak at 28.5°. The crystalline particle size changed in the range of 6.6–10.8 nm, which has a close relationship with the DI-H_2O amount in the solvent. The CeO_2-H0 sample, prepared without extra DI-H_2O, possessed the biggest crystalline particle size of 10.8 nm. By adding extra DI-H_2O to the precursor solution, the crystalline particle size decreased first (1–3 ml DI-H_2O) and then increased again (4–5 ml DI-H_2O). The smallest crystalline particle (6.6 nm) appeared when the extra DI-H_2O was 3 ml (CeO_2-H3).

The groups on the particle surfaces were characterized by FT-IR (**Figure 2B**). After calcination at 500°C for 1 h, most of the organic groups were removed, and only a small amount of C=O (1,300–1,650 cm^{-1}) and C-O (1,060 cm^{-1}) groups can be observed besides the OH group at c.a. 3,500 cm^{-1} (Guo et al., 2021), indicating a relatively clean surface. These groups may be caused by the adsorption of CO_2 and H_2O from the air, which can be further confirmed by XPS results in **Figure 5**.

The DI-H_2O amount in the solvent can influence the morphologies of CeO_2 particles, as shown in **Figure 3**. When there was no extra H_2O in the solution, the CeO_2-H0 sample (**Figure 3A**) exhibited an octahedral shape

TABLE 1 | Reagents used for different sample syntheses.

Sample	$Ce(NO_3)_3{\cdot}6H_2O$ (g)	PVP (g)	HAC (ml)	EG (ml)	DI-H_2O (ml)
CeO_2-H0	2.17	1.00	2.0	35.0	0
CeO_2-H1	2.17	1.00	2.0	34.0	1.0
CeO_2-H2	2.17	1.00	2.0	33.0	2.0
CeO_2-H3	2.17	1.00	2.0	32.0	3.0
CeO_2-H4	2.17	1.00	2.0	31.0	4.0
CeO_2-H5	2.17	1.00	2.0	30.0	5.0

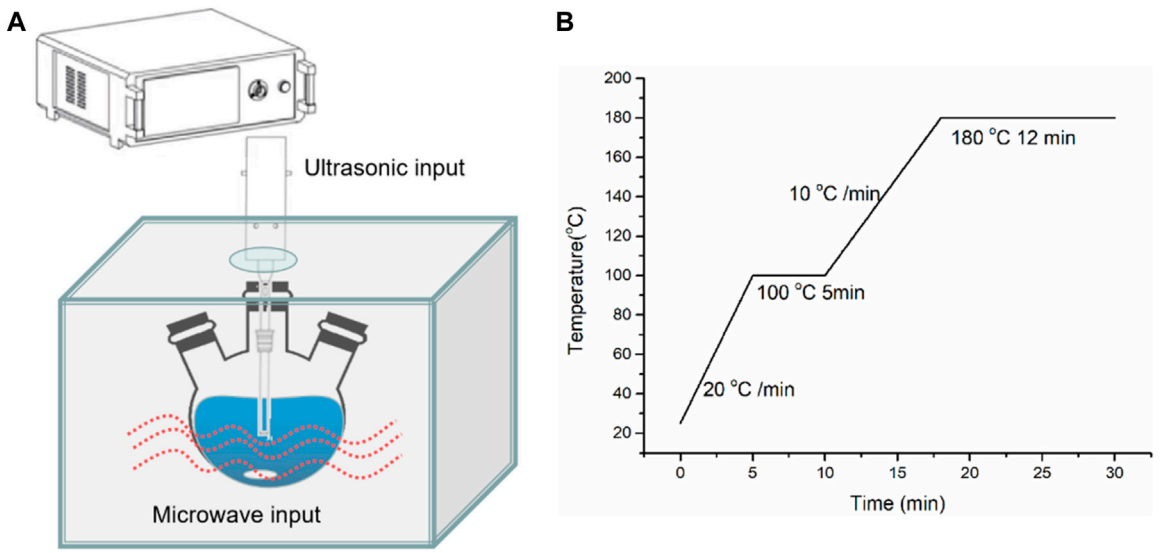

FIGURE 1 | Sketch of combined microwave–ultrasonic synthesis **(A)** and heating program **(B)**.

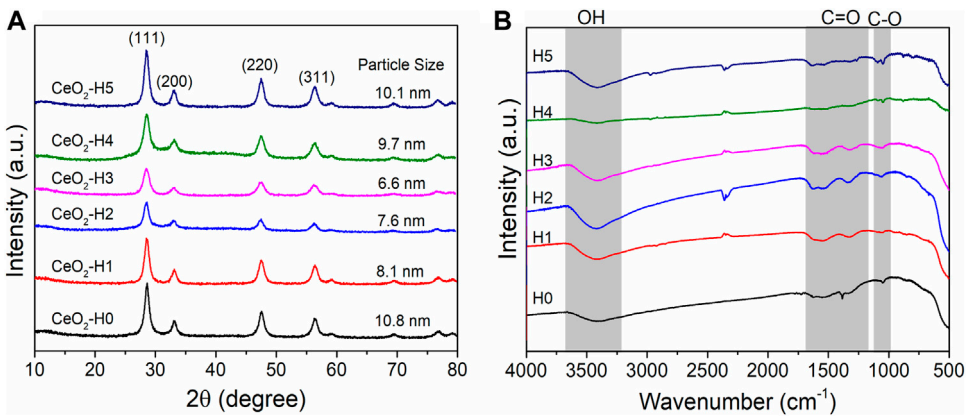

FIGURE 2 | XRD **(A)** and IR **(B)** spectra of CeO_2 by the combined microwave–ultrasonic method and calcined at 500°C in air for 1 h. The particle sizes in **(A)** are calculated by Scherrer equations based on the strongest peak at 28.5°.

(diameter: 280 nm, length: 460 nm, and aspect ratio: 1.6), formed by aggregation of nanoparticles. The CeO_2-H1 sample (**Figure 3B**), with 1 ml extra DI-H_2O in the solution, also showed a roughly octahedron structure, much more like a shuttle shape (diameter: 180 nm, length: 380 nm, and aspect ratio: 2), and small particles became more obvious in the aggregate. CeO_2-H2 (**Figure 3C**) possessed a similar structure to CeO_2-H1; only the diameter became smaller, which was about 140 nm. When increasing H_2O to 3 ml, CeO_2-H3 (**Figure 3D**) showed a smaller aggregation

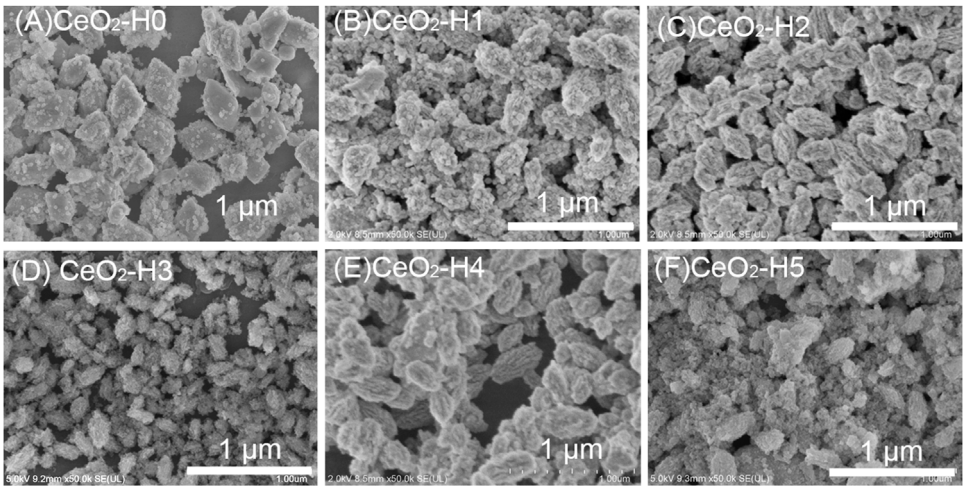

FIGURE 3 | SEM morphologies of CeO_2 prepared by the combined microwave–ultrasonic method and calcined at 500°C in air for 1 h. **(A)** CeO_2-H0, **(B)** CeO_2-H1, **(C)** CeO_2-H2, **(D)** CeO_2-H3, **(E)** CeO_2-H4, **(F)** CeO_2-H5.

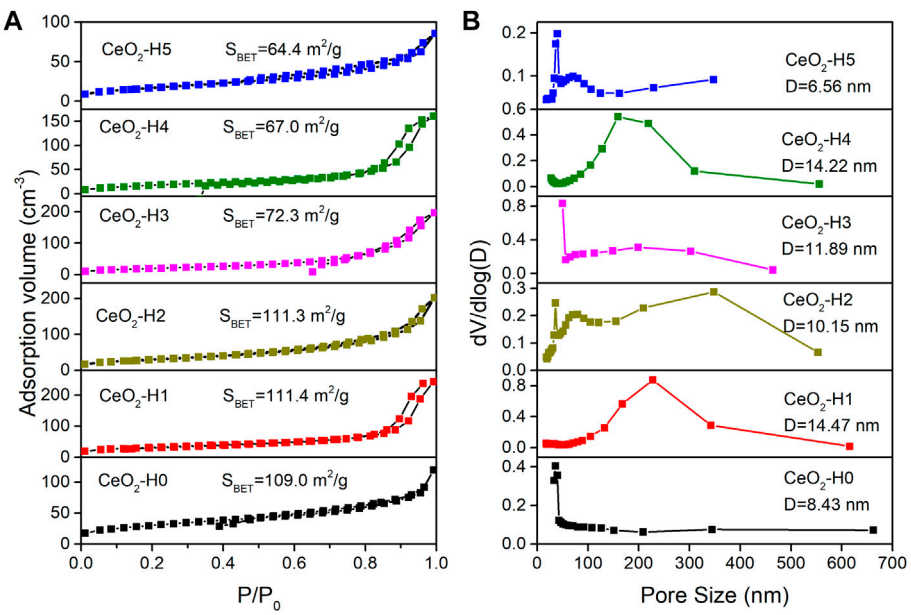

FIGURE 4 | N_2 sorption isotherm **(A)** and pore size distribution **(B)** of CeO_2 prepared by the combined microwave–ultrasonic method and calcined at 500°C in air for 1 h.

structure, with a diameter of 80 nm and length of 200 nm (aspect ratio: 2.5). By further increasing H_2O to 4 ml, the size of the aggregate in CeO_2-H4 (**Figure 3E**) increased again, exhibiting a structure similar to that of samples CeO_2-H1 and CeO_2-H2. Nevertheless, the octahedron/shuttle shape collapsed for CeO_2-H5 (**Figure 3F**); most were small particles, and only few aggregates can be observed. CeO_2 shuttles were previously synthesized by the hydrothermal method under similar conditions (Guo et al., 2008), but the size (diameter: 800 nm) was much larger than that of the samples in this work.

The N_2 adsorption–desorption isotherm is used to characterize the materials' surface area, as shown in **Figure 4A**, and the pore diameter distribution is shown in **Figure 4B**. According to the IUPAC classification (Sing et al., 1985; Yang et al., 2020c; Zhang et al., 2021), the hysteresis loop of

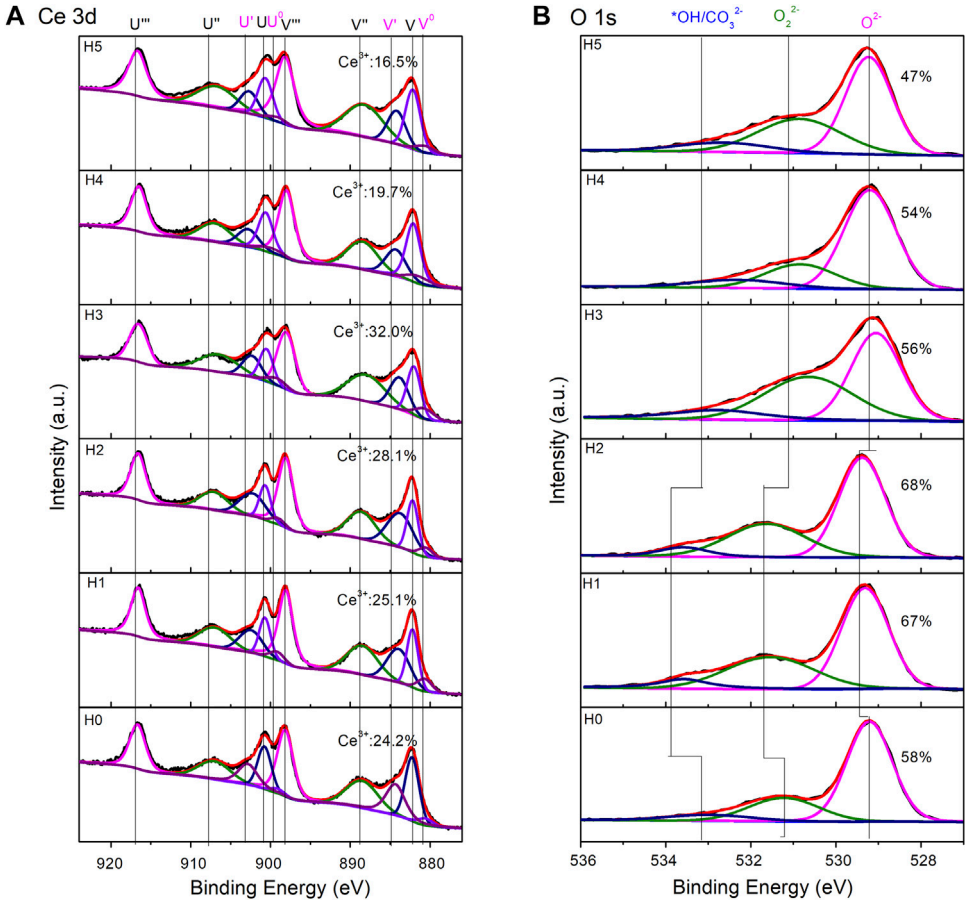

FIGURE 5 | XP spectra of CeO_2 by the combined microwave–ultrasonic method and calcined at 500°C in air for 1 h. **(A)** is the region of Ce 3d, in which V^0, V′, U^0, and U′ belong to Ce^{3+}. **(B)** is the region of O 1 s.

the N_2 adsorption isotherm belonged to type VI, indicating that the materials were mesoporous. The specific surface area of CeO_2-H2 (S_{BET}: 111.3 m^2/g) was similar to that of CeO_2-H1 (S_{BET}: 111.4 m^2/g), larger than the values of other samples, while the minimum S_{BET} (64.4 m^2/g) belonged to CeO_2-H5. Besides the surface area, the H_2O amount also influenced the pore size distribution, as shown in **Figure 4B**. When there was no additional H_2O added (sample CeO_2-H0), the pore size distribution was relatively narrow, and almost all pore sizes were below 10 nm. When H_2O was added to the system, the pore size distribution became broader, especially for sample CeO_2-H2. This confirmed that adding H_2O can influence the samples' morphologies. This may be related to the change in the PVP micelle structure. The extra H_2O addition to the synthesis system changed the arrangement of PVP, resulting in the agglomeration alternation in CeO_2 particles, and the shape of CeO_2 became irregular along with H_2O addition, as shown in **Figure 3** and illustrated in **Figure 6**. The agglomeration variations in CeO_2 particles presented a different surface area and pore size distribution.

XPS is used to characterize the CeO_2 surface states (**Figure 5**). Ce^{3+} defects are important and have a close relationship with the catalytic activity of CeO_2. In the Ce3d region (**Figure 5A**), Ce^{3+} ratios were calculated using the previous method, by fitting the area of Ce^{3+} and Ce^{4+} peaks (Zhang et al., 2017; Yang et al., 2018; Yang et al., 2020a). The CeO_2-H0 sample had a Ce^{3+} ratio of 24.2%. The addition of H_2O increased the Ce^{3+} ratio first and then decreased the number of Ce^{3+} defects. The highest Ce^{3+} ratio (32.0%) belonged to the CeO_2-H3 sample, with 3 ml H_2O added to the synthesizing system. CeO_2-H2 possessed a Ce^{3+} ratio of 28.1%, which was the second top of all Ce^{3+} ratios. Besides, the O1s region can be fitted into three peaks: OH^*/CO_3^{2-}, O_2^{2-}, and O^{2-} (Chen et al., 2013). OH^*/CO_3^{2-} and O_2^{2-} were normally caused by the organic residuals or the surface impurity caused by CO_2 and H_2O adsorption, and they can block the active sites of CeO_2 (Ferreira et al., 2012; Jiang et al., 2015; Yang et al., 2018). Thus, the higher the O^{2-} ratio is, the cleaner the CeO_2 surface is, indicating more active sites can be exposed. From the O1s region in **Figure 5B**, it can be seen that the CeO_2-H2 sample possessed the highest O^{2-} ratio (68%), suggesting that it has the cleanest surface, which is beneficial to the catalytic activity. The highest O^{2-} ratio of CeO_2-H2 may be because a suitable amount of H_2O promoted the cleavage of organic residuals, as illustrated in **Figure 6**. This may compensate the slightly lower Ce^{3+} ratio

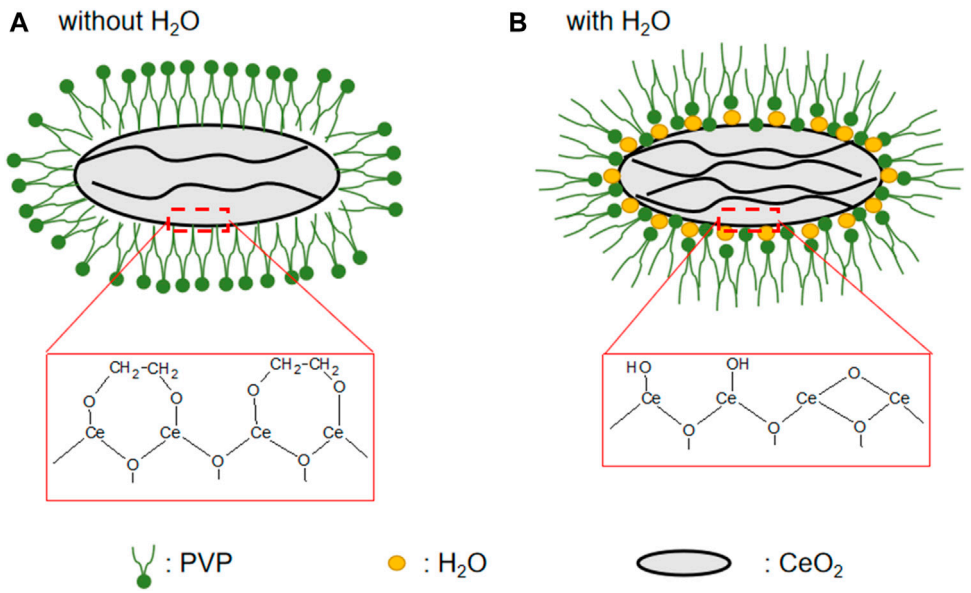

FIGURE 6 | Sketch of the influence of H_2O on the structure of CeO_2. **(A)** Without H_2O. **(B)** With H_2O.

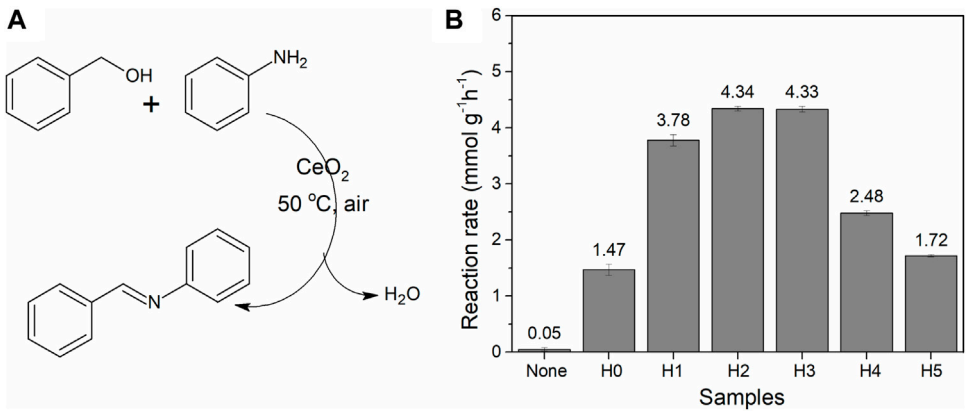

FIGURE 7 | (A) Reaction for imine synthesis. **(B)** Imine conversion of CeO_2 (50 mg) synthesized in different amounts of water (amount of catalyst per hour; all values of conversion are calculated below 20%). The experiment was repeated three times, and the average conversion value was given with an error bar.

of the CeO_2-H2 sample, resulting in the highest catalytic activity for imine synthesis, as shown in **Figure 7**.

From the above-mentioned characterization, the addition of H_2O can change the morphology of CeO_2, which can further alter the specific surface area and the surface Ce^{3+} defects. These changes may be related to the PVP micelle structure change and the CeO_2 surface coordination state induced by H_2O, as sketched in **Figure 6**. When no H_2O is added to the system, the CeO_2 surface is covered with EG molecules, and the surface is hydrophobic. Thus, the PVP formed a micelle structure, with the hydrophobic ends toward the CeO_2 agglomeration particles. When H_2O is added to the system, it can react with the Ce-precursor, forming a Ce-OH structure; thus, the CeO_2 surface transformed from hydrophobic to hydrophilic, and the PVP formed a micelle structure, with the hydrophilic ends toward to the CeO_2 particles. Besides, Ce-OH can also yield a cleaner surface, and the condensation between -OH can happen to yield oxygen vacancies and H_2O, yielding a higher Ce^{3+} ratio. Meanwhile, H_2O can also be adsorbed onto the CeO_2 surface, which can interact with the microwave and sonic energy much better than EG can, causing more wrinkles on the CeO_2 particles to increase the specific surface area. However, when more than 4 ml of H_2O was added into the system, the PVP micelle structure was destroyed, and no shuttle structure can be observed.

When synthesized CeO_2 was used for imine synthesis, they exhibit different activities (**Figure 7**). The order of imine

conversion is CeO_2-H2 (4.34 mmol g^{-1} h^{-1}) ≈ CeO_2-H3 (4.33 mmol g^{-1} h^{-1}) > CeO_2-H1 (3.78 mmol g^{-1} h^{-1}) > CeO_2-H4 (2.48 mmol g^{-1} h^{-1}) > CeO_2-H5 (1.72 mmol g^{-1} h^{-1}) > CeO_2-H0 (1.47 mmol g^{-1} h^{-1}). The reaction rates of all the samples were far better than the 0.46 mmol g^{-1} h^{-1} reported in Angew (Tamura and Tomishige, 2015). It has been reported earlier that CeO_2 can be used as an easily separable catalyst for imine synthesis at low temperature (<100°C) (Zhang et al., 2017; Zhang et al., 2018; Chen et al., 2020; Wu et al., 2021) and oxygen vacancies (Ce^{3+} defects) played an important role during this reaction. The Ce^{3+} vacancies can promote the transition of benzyl alcohol to benzaldehyde, and the latter can easily couple with aniline to form an imine compound (Tamura and Tomishige, 2015; Zhang et al., 2017; Qin et al., 2019). From the above-mentioned results, it can be seen that CeO_2-H2 possessed the largest surface area (111.4 m^2/g) and a relatively high Ce^{3+} ratio (28.1%), which contributed to the highest imine reaction rate. CeO_2-H3 exhibited a similar catalytic activity, which may be due to its highest Ce^{3+} ratio (32.0%), but its surface area (72.3 m^2/g) is a little bit lower than that of CeO_2-H2. The results confirmed that both surface area and Ce^{3+} ratio are important to the CeO_2 catalytic properties for imine synthesis.

CONCLUSION

Different sizes of fusiform CeO_2 were synthesized by the combined microwave–ultrasonic method, and H_2O was added to change the structure of CeO_2. By changing the amount of H_2O from 1 to 5 ml, the specific surface area of CeO_2 changed from 111 m^2/g to 64 m^2/g, while the Ce^{3+} ratio varied in the range of 16.5% and 32.0%. The sample with 2 ml H_2O has the largest surface area (111.4 m^2/g) and a relatively high Ce^{3+} ratio (28.1%), indicating that the CeO_2-H2 sample has the largest amount of exposed surface oxygen vacancies, and the imine reaction rate is 4.34 mmol g^{-1} h^{-1}, which is almost three times the rate (1.47 mmol g^{-1} h^{-1}) produced by the sample without addition of water.

DATA AVAILABILITY STATEMENT

The original contributions presented in the study are included in the article/Supplementary Material; further inquiries can be directed to the corresponding author.

AUTHOR CONTRIBUTIONS

XC and JY conceived this work, HD collected the data. XC wrote the original manuscript, and JY reviewed and edited the manuscript.

FUNDING

This research was supported by the National Natural Science Foundation of China (Grant No. 12175035).

REFERENCES

Cao, X., Qin, J., Gou, G., Li, J., Wu, W., Luo, S., et al. (2020). Continuous Solvent-free Synthesis of Imines over Uip-γ-Al2O3-CeO2 Catalyst in a Fixed Bed Reactor. *Appl. Catal. B Environ.* 272, 118958. doi:10.1016/j.apcatb.2020.118958

Chen, B., Ma, Y., Ding, L., Xu, L., Wu, Z., Yuan, Q., et al. (2013). Reactivity of Hydroxyls and Water on a CeO2(111) Thin Film Surface: The Role of Oxygen Vacancy. *J. Phys. Chem. C* 117, 5800–5810. doi:10.1021/jp312406f

Chen, H., Shen, J., and Zhang, Y. (2021). Nanocomposite Synthesis of MoS2/nano-CeO2 for High-Performance Electromagnetic Absorption. *J. Mat. Sci. Mat. Electron.* 32, 22689–22698. doi:10.1007/s10854-021-06755-z

Chen, L.-Y., Xu, F.-F., Zhang, J., Ding, H., and Yang, J. (2020). Structure Design of CeO2-MoS2 Composites and Their Efficient Activity for Imine Synthesis. *Appl. Nanosci.* 10, 233–241. doi:10.1007/s13204-019-01114-1

Dalas, E. (2001). The Effect of Ultrasonic Field on Calcium Carbonate Scale Formation. *J. Cryst. Growth* 222, 287–292. doi:10.1016/S0022-0248(00)00895-2

Ferreira, V. J., Tavares, P., Figueiredo, J. L., and Faria, J. L. (2012). Effect of Mg, Ca, and Sr on CeO2 Based Catalysts for the Oxidative Coupling of Methane: Investigation on the Oxygen Species Responsible for Catalytic Performance. *Ind. Eng. Chem. Res.* 51, 10535–10541. doi:10.1021/ie3001953

Geng, L., Song, J., Zhou, Y., Xie, Y., Huang, J., Zhang, W., et al. (2016). CeO2 Nanorods Anchored on Mesoporous Carbon as an Efficient Catalyst for Imine Synthesis. *Chem. Commun.* 52, 13495–13498. doi:10.1039/c6cc05496j

Guo, L., Yang, J., Zhang, H., Wang, R., Xu, J., and Wang, J. (2021). Highly Enhanced Visible-light Photocatalytic Activity via a Novel Surface Structure of CeO 2 /g–C 3 N 4 toward Removal of 2,4-dichlorophenol and Cr(VI). *ChemCatChem* 13, 2034–2044. doi:10.1002/cctc.202001939

Guo, Z., Du, F., Li, G., and Cui, Z. (2008). Synthesis of Single-Crystalline CeCO3OH with Shuttle Morphology and Their Thermal Conversion to CeO2. *Cryst. Growth & Des.* 8, 2674–2677. doi:10.1021/cg070556z

Jiang, D., Wang, W., Zhang, L., Qiu, R., Sun, S., and Zheng, Y. (2015). A Strategy for Improving Deactivation of Catalytic Combustion at Low Temperature via Synergistic Photocatalysis. *Appl. Catal. B Environ.* 165, 399–407. doi:10.1016/j.apcatb.2014.10.040

Kaldas, S. J., O'keefe, K. T. V., Mendoza-Sanchez, R., and Yudin, A. K. (2017). Amphoteric Borylketenimines: Versatile Intermediates in the Synthesis of Borylated Heterocycles. *Chem. Eur. J.* 23, 9711–9715. doi:10.1002/chem.201702008

Leonelli, C., and Mason, T. J. (2010). Microwave and Ultrasonic Processing: Now a Realistic Option for Industry. *Chem. Eng. Process. Process Intensif.* 49, 885–900. doi:10.1016/j.cep.2010.05.006

Li, Y., Lu, Y.-L., Wu, K.-D., Zhang, D.-Z., Debliquy, M., and Zhang, C. (2021). Microwave-Assisted Hydrothermal Synthesis of Copper Oxide-Based Gas-Sensitive Nanostructures. *Rare Met.* 40, 1477–1493. doi:10.1007/s12598-020-01557-4

Long, Y., Gao, Z., Qin, J., Wang, P., Wu, W., Zhang, L., et al. (2019a). CeO2 Immobilized on Magnetic Core-Shell Microparticles for One-Pot Synthesis of Imines from Benzyl Alcohols and Anilines: Support Effects for Activity and Stability. *J. Colloid Interface Sci.* 538, 709–719. doi:10.1016/j.jcis.2018.11.092

Long, Y., Zhang, H., Gao, Z., Qin, J., Pan, Y., Zhao, J., et al. (2019b). A Protective Roasting Strategy for Preparation of Stable Mesoporous Hollow CeO2 Microspheres with Enhanced Catalytic Activity for One-Pot Synthesis of Imines from Benzyl Alcohols and Anilines. *Inorg. Chem. Front.* 6, 829–836. doi:10.1039/c9qi00024k

Ma, X., Zhang, X.-Y., Yang, M., Martin, S. F., Xie, J.-Y., Lv, R.-Q., and Chai, Y.-M. (2021). High-Pressure Microwave-Assisted Synthesis of WSx/Ni9S8/NF

Hetero-Catalyst for Efficient Oxygen Evolution Reaction. *Rare Met.* 40, 1048–1055. doi:10.1007/s12598-020-01704-x

Martin, S. F. (2009). Recent Applications of Imines as Key Intermediates in the Synthesis of Alkaloids and Novel Nitrogen Heterocycles. *Pure Appl. Chem.* 81, 195–204. doi:10.1351/PAC-CON-08-07-03

Mousavi-Kamazani, M., and Ashrafi, S. (2020). Single-step Sonochemical Synthesis of Cu2O-CeO2 Nanocomposites with Enhanced Photocatalytic Oxidative Desulfurization. *Ultrason. Sonochemistry* 63, 104948. doi:10.1016/j.ultsonch.2019.104948

Phuruangrat, A., Thongtem, S., and Thongtem, T. (2017). Microwave-assisted Hydrothermal Synthesis and Characterization of CeO2 Nanowires for Using as a Photocatalytic Material. *Mater. Lett.* 196, 61–63. doi:10.1016/j.matlet.2017.03.013

Qin, J., Long, Y., Wu, W., Zhang, W., Gao, Z., and Ma, J. (2019). Amorphous Fe2O3 Improved [O] Transfer Cycle of Ce4+/Ce3+ in CeO2 for Atom Economy Synthesis of Imines at Low Temperature. *J. Catal.* 371, 161–174. doi:10.1016/j.jcat.2019.01.032

Reddy, L. H., Reddy, G. K., Devaiah, D., and Reddy, B. M. (2012). A Rapid Microwave-Assisted Solution Combustion Synthesis of CuO Promoted CeO2-MxOy (M=Zr, La, Pr and Sm) Catalysts for CO Oxidation. *Appl. Catal. A General* 445-446, 297–305. doi:10.1016/j.apcata.2012.08.024

Rizzuti, A., Dipalo, M. C., Allegretta, I., Terzano, R., Cioffi, N., Mastrorilli, P., et al. (2020). Microwave-Assisted Solvothermal Synthesis of Fe3O4/CeO2 Nanocomposites and Their Catalytic Activity in the Imine Formation from Benzyl Alcohol and Aniline. *Catalysts* 10, 1325. doi:10.3390/catal10111325

Shen, X.-F. (2009). Combining Microwave and Ultrasound Irradiation for Rapid Synthesis of Nanowires: a Case Study on Pb(OH)Br. *J. Chem. Technol. Biotechnol.* 84, 1811–1817. doi:10.1002/jctb.2250

Sing, K. S. W., Everett, D. H., Haul, R. a. W., and Moscou, L. R. A. (1985). Reporting Physisorption Data for Gas/solid Systems with Special Reference to the Determination of Surface Area and Porosity (Recommendations 1984). *Pure Appl. Chem.* 57, 603–619. doi:10.1351/pac19825411220110.1351/pac198557040603

Tamura, M., and Tomishige, K. (2015). Redox Properties of CeO2at Low Temperature: The Direct Synthesis of Imines from Alcohol and Amine. *Angew. Chem. Int. Ed.* 54, 864–867. doi:10.1002/anie.201409601

Tamura, M., and Tomishige, K. (2020). Scope and Reaction Mechanism of CeO2-Catalyzed One-Pot Imine Synthesis from Alcohols and Amines. *J. Catal.* 389, 285–296. doi:10.1016/j.jcat.2020.05.031

Thompson, L. H., and Doraiswamy, L. K. (2000). The Rate Enhancing Effect of Ultrasound by Inducing Supersaturation in a Solid-Liquid System. *Chem. Eng. Sci.* 55, 3085–3090. doi:10.1016/S0009-2509(99)00481-9

Wu, S., Wang, Y., Cao, Q., Zhao, Q., and Fang, W. (2021). Efficient Imine Formation by Oxidative Coupling at Low Temperature Catalyzed by High-Surface-Area Mesoporous CeO 2 with Exceptional Redox Property. *Chem. Eur. J.* 27, 3019–3028. doi:10.1002/chem.202003915

Yang, J., Ding, H., Wang, J., Yigit, N., Xu, J., Rupprechter, G., et al. (2020a). Energy-Guided Shape Control towards Highly Active CeO2. *Top. Catal.* 63, 1743–1753. doi:10.1007/s11244-020-01357-1

Yang, J., Ding, H., Zhu, Z., Wang, Q., Wang, J., Xu, J., et al. (2018). Surface Modification of CeO2 Nanoflakes by Low Temperature Plasma Treatment to Enhance Imine Yield: Influences of Different Plasma Atmospheres. *Appl. Surf. Sci.* 454, 173–180. doi:10.1016/j.apsusc.2018.05.135

Yang, J., Peng, S., Shi, Y., Ma, S., Ding, H., Rupprechter, G., et al. (2020b). Fast Visual Evaluation of the Catalytic Activity of CeO2: Simple Colorimetric Assay Using 3,3′,5,5′-tetramethylbenzidine as Indicator. *J. Catal.* 389, 71–77. doi:10.1016/j.jcat.2020.05.016

Yang, J., Yigit, N., Möller, J., and Rupprechter, G. (2021). Co 3 O 4 –CeO 2 Nanocomposites for Low-Temperature CO Oxidation. *Chem. A Eur. J.* 27, 16947–16955. doi:10.1002/chem.202100927

Yang, J., Zhang, J., Zou, B., Zhang, H., Wang, J., Schubert, U., et al. (2020c). Black SnO2-TiO2 Nanocomposites with High Dispersion for Photocatalytic and Photovoltaic Applications. *ACS Appl. Nano Mat.* 3, 4265–4273. doi:10.1021/acsanm.0c00432

Zhai, Y., Xin, G., Wang, J., Zhang, B., Song, J., and Liu, X. (2021). Microwave-assisted Synthesis of rGO/CeO2 Supercapacitor Electrode Materials with Excellent Electrochemical Properties. *Acta Chim. Sin.* 79, 1129–1137. doi:10.6023/a21050216

Zhang, H., Wu, C., Wang, W., Bu, J., Zhou, F., Zhang, B., et al. (2018). Effect of Ceria on Redox-Catalytic Property in Mild Condition: A Solvent-free Route for Imine Synthesis at Low Temperature. *Appl. Catal. B Environ.* 227, 209–217. doi:10.1016/j.apcatb.2018.01.012

Zhang, H., Yang, J., Guo, L., Wang, R., Peng, S., Wang, J., et al. (2021). Microwave-aided Synthesis of BiOI/g-C3n4 Composites and Their Enhanced Catalytic Activities for Cr(VI) Removal. *Chem. Phys. Lett.* 762, 138143. doi:10.1016/j.cplett.2020.138143

Zhang, J., Yang, J., Wang, J., Ding, H., Liu, Q., Schubert, U., et al. (2017). Surface Oxygen Vacancies Dominated CeO2 as Efficient Catalyst for Imine Synthesis: Influences of Different Cerium Precursors. *Mol. Catal.* 443, 131–138. doi:10.1016/j.mcat.2017.09.030

Zhao, P. S., Gao, X. M., Zhu, F. X., Hu, X. M., and Zhang, L. L. (2018). Ultrasonic-assisted Solution-phase Synthesis and Property Studies of Hierarchical Layer-By-Layer Mesoporous CeO2. *Bull. Korean Chem. Soc.* 39, 375–380. doi:10.1002/bkcs.11398

Conflict of Interest: The authors declare that the research was conducted in the absence of any commercial or financial relationships that could be construed as a potential conflict of interest.

Publisher's Note: All claims expressed in this article are solely those of the authors and do not necessarily represent those of their affiliated organizations, or those of the publisher, the editors, and the reviewers. Any product that may be evaluated in this article, or claim that may be made by its manufacturer, is not guaranteed or endorsed by the publisher.